Optimal design of adsorption chillers based on a validated dynamic object-oriented model

The design of adsorption chillers is usually based on experience and high experimental effort. Experimental effort can be reduced by using dynamic models. In the present study, a dynamic model is validated with a modular adsorption chiller test-bed and then used to optimize design and process parameters to gain maximum cooling power. The modularity of the test bed enables the exchange of single components, without changing the remaining setup. This modular structure is also reflected in the object-oriented dynamic model. Model calibration is based on the heat flows of all components. This measure allows to gain deep insight into the system behavior and a quantitative comparison of model accuracy. The calibrated model is validated by predicting the system behavior for different operating conditions and also changed adsorbent materials. Adsorbent materials silica gel 123 and zeolite 13X are investigated. Operating points vary in cycle time, as well as temperatures of evaporation, adsorption and desorption. The model exhibits excellent prediction capability for the coefficient of performance and for the cooling power. The modular setup of the model is then used for targeted optimization of the adsorption system: the cycle time and the sizing of the heat exchangers are rigorously optimized leading to adsorption chillers with maximum cooling power.

Introduction

Adsorption chillers can provide cold in an environmental friendly way by using waste heat or solar irradiation as driving energy. The design and development of adsorption chillers is challenging due to the cyclic operation and the highly dynamic behavior. This usually leads to high experimental effort and requires longtime experience.

To support the development of adsorption chillers with simulation, dynamic computer models are increasingly employed. Since many of the used models are not experimentally validated, e.g. (Miyazaki et al. 2010), (Farid et al. 2011), (Santori et al. 2012) and (Tso et al. 2012), the reliability and accuracy of the simulation results are unknown. Confidence in the simulation results for specific operation points can be achieved by calibration of the models with measurements. Early work on this field was done by Douss et al.

Science and Technology for the Built Environment (2015) 21, 248–257
DOI: 10.1080/10789669.2014.990337

(1988) and Saha et al. (1995), and more recent model calibrations were conducted by Verde et al. (2010) and Zhang et al. (2011). While good descriptions of experiments were achieved, quantification of the model accuracy remains difficult. Schicktanz and Nunez (2009) quantify model accuracy by using the normalized standard deviation between simulated and measured temperature and pressure curves.

The models are usually calibrated at a single operation point, i.e. fixed temperatures and cycle times. Wang and Chua (2007a, 2007b), on the contrary, validated their models at different operating conditions, but their models still exhibit large prediction errors up to 50 %. Chen et al. (2010) demonstrated that their model could be used to predict process performance within a limited range of process conditions.

The overall design of adsorption chillers has been considered in several parametric studies, e.g. (Saha et al. 2006), (Khan et al. 2006) and (Khan et al. 2007). These studies analyzed the dependence of *COP* (coefficient of performance) and cooling power on the overall thermal conductance of the heat exchangers, the heat capacity and the sorbent mass.

In this work, we present a model that is not only valid for a broad range of operating conditions but also for different setups, i.e. different adsorbent materials and heat exchanger capacities. The dynamic object-oriented model was tested with a modular and flexible experimental setup. First, the model parameters were calibrated at one specific operation point and subsequently validated for different boundary temperatures and cycle times. Additionally, the experimental setup was modified by changing the adsorbent material and the heat transfer ability of the evaporator. The model allows reliable prediction of the performance for the modified setup after calibration of the affected parameters. The accuracy of the model is mathematically quantified for all cases studied, confirming the high prediction capability. The validated model is then used to improve the adsorption chiller design: The sizing of the single components (adsorber, evaporator and condenser) and the cycle time are concurrently optimized for a fixed total volume of the adsorption chiller. Thereby, the presented approach can be used to derive practical design guidelines to optimize the cooling power of real adsorption systems.

In the next section, we present the dynamic model of the adsorption chiller, followed by the experimental setup which is used to validate the model. Afterwards the model calibration and validation is described. In the last section, the adsorption chiller is optimized with respect to cycle time and heat exchanger sizing.

Model

The adsorption chiller model is written in the object-oriented modeling language Modelica (Fritzson 2004). Modelica allows dynamic process simulation, which is essential for the cyclic behavior of adsorption systems without steady-states. In addition, the TIL and TILMedia library (Gräber et al. 2010) is used to model heat exchangers and fluid properties.

We have developed a Modelica library for adsorption based energy systems (Bau et al. 2014). The object-oriented models of our library reflect the modular structure of adsorption chillers. Thereby, the library enables flexible modeling of different setups and quick adaption of heat and mass transfer models.

In this work, the adsorption chiller model consists of one adsorber bed that is connected via valves to an evaporator and condenser (Figure 1). An additional water reservoir provides constant filling levels in evaporator and condenser. The configuration of the model is according to the experimental setup in our laboratory.

Some general assumptions are made to reduce modelling complexity:

- All units are lumped models with uniform properties.
- Only the heat exchanger tubes of adsorber, condenser and evaporator have 1D-discretization.
- There is no direct heat transfer between adsorber, condenser and evaporator.
- There are no heat losses to the ambient.
- There are neither leakages nor inert gases.
- The heat capacities of the vacuum vessels are neglected.

Adsorber

Central unit of the model is the adsorber. The adsorber model contains mass and energy balances with adjustable transfer coefficients (Figure 1). Within the adsorber model, the equilibrium data of the working pair is computed by an exchangeable adsorption equilibrium model. The equilibrium model employed in this work is the Dubinin model (Dubinin 1967). The Dubinin model calculates the internal energy u_{ad} and the pressure p_{ad} of the adsorbed phase (ad) as function of loading x and temperature T of the sorbent (sor) using a characteristic function for the employed working pair. In the present work, the characteristic functions of the working pairs silica gel 123 - water (Schawe 2001) and zeolite 13X - water (own experimental data) are used. The density ρ_{ad} and heat capacity c_{ad} of the adsorbed water is assumed to be equal to that of liquid

water and obtained from TILMedia library. The sorbent is modelled jointly with the adsorbed water as a lumped model with uniform temperature T, loading x and pressure p_{ad}.

The mass balance for the sorbent reads

$$m_{\mathrm{sor}} \frac{dx}{dt} = \frac{dm_{\mathrm{ad}}}{dt} = \dot{m} \,, \tag{1}$$

where the mass flow $\dot{m}$ to and from the sorbent is governed by a linear driving force (LDF) approach suggested by Glueckauf (1955) for spherical pellets:

$$\dot{m} = \frac{15\, m_{\mathrm{sor}}}{r_{\mathrm{sor}}^2}\, D \left[x_{\mathrm{eq}}(p_{\mathrm{A}}) - x(p_{\mathrm{ad}}) \right] . \tag{2}$$

The mass flow $\dot{m}$ is proportional to a diffusion coefficient D and the difference between the actual loading $x(p_{\mathrm{ad}})$ of the sorbent and the equilibrium loading x_{eq} at pressure p_{A} of the surrounding vapor in the adsorber. For the adsorption (ads) and desorption (des) phase, the diffusion coefficient D can take different values and serves as a fitting parameter in the later model calibration below. The prefactor in equation (2) contains the sorbent mass m_{sor} and the sorbent radius r_{sor}.

The energy balance for the sorbent is given by:

$$\frac{\mathrm{d}U}{\mathrm{d}t} = u_{\mathrm{ad}} \frac{\mathrm{d}m_{\mathrm{ad}}}{\mathrm{d}t} + (m_{\mathrm{ad}} c_{\mathrm{ad}} + m_{\mathrm{sor}} c_{\mathrm{sor}}) \frac{\mathrm{d}T}{\mathrm{d}t} = \dot{H} + \dot{Q} \,. \tag{3}$$

The internal energy U is affected by the change of the amount of adsorbed water m_{ad} as well as by temperature changes of both the adsorbed water (ad) and the sorbent, with dry sorbent mass m_{sor} and heat capacity c_{sor}. For desorption processes, the enthalpy flow $\dot{H} = \dot{m} h_{\mathrm{v}}$ is calculated with the specific enthalpy h_{v} of water vapor at temperature T and pressure p_{ad} of the sorbent. The heat flow

$$\dot{Q} = (\alpha A)_{\mathrm{A}} \cdot \Delta T \tag{4}$$

between sorbent and the outer heat exchanger surface is described with a constant heat transfer coefficient $(\alpha A)_{\mathrm{A}}$ that is used as calibration parameter as well. The heat exchangers are the only models with a one dimensional discretization to allow modelling of temperature gradients in flow direction of the heat exchangers tubes. In this work, heat exchanger models for plain tubes from the TIL library are used. The convective heat transfer inside the tubes is calculated with the Sieder-Tate correlation (Thome 2010) and heat conduction in the wall is also considered.

Condenser and evaporator

Condenser (C) and evaporator (E) models have the same structure as the adsorber model except for the equilibrium model, which is replaced by a vapor-liquid-equilibrium model for water from TILMedia library. The mass and energy balances are

$$\frac{\mathrm{d}m}{\mathrm{d}t} = \dot{m}_{\mathrm{v}} + \dot{m}_{\mathrm{l}}\,, \tag{5}$$

$$\frac{dU}{dt} = \dot{H}_{\mathrm{v}} + \dot{H}_{\mathrm{l}} + \dot{Q}\,. \tag{6}$$

Water can be exchanged via vapor (v) and liquid (l) ports. At the vapor port, the water leaves as saturated vapor, at the liquid port as saturated liquid. The heat flow $\dot{Q}$ between saturated water in the evaporator/condenser and heat exchanger surface

$$\dot{Q} = (\alpha A)_{\mathrm{E/C}} \cdot \Delta T \tag{7}$$

is accordingly described with constant heat transfer coefficients $(\alpha A)_{\mathrm{E/C}}$. The constant coefficients are a simplification of the occurring heat transfer phenomena and thus not strictly valid, but accurately enough to describe the heat pump behavior (cf. section: model calibration). Both heat transfer coefficients $(\alpha A)_{\mathrm{E/C}}$ are also fitting parameters for the model calibration. The convective heat transfer inside the tubes is calculated with the Sieder-Tate correlation for the straight tubes (Thome 2010) in the evaporator and the Schmidt correlation for the condenser helix (Schmidt 1967).

Valves

A laminar flow is assumed in the pipes and valves between the vacuum vessels of adsorber, evaporator and condenser and the pressure drop Δp is calculated as follows:

$$\Delta p = f\ \mu\ v\,. \tag{8}$$

The pressure drop is directly proportional to the velocity v and the dynamic viscosity μ of the steam (similar to the Hagen-Poiseuille equation). The friction factor f is used as a fitting parameter for the model. The valve model does not contain any storage terms for mass and energy.

Experimental setup

The experimental setup has the same structure as the model consisting of one adsorber, evaporator, condenser and an additional water reservoir. To get an impression of the single units, the heat exchangers are shown in Figure 2.

The heat exchanger of the adsorber consists of extruded aluminum tubes connected in series. To enhance the convective heat transfer of the inner water circuit, the tubes have an inner fin structure. The outer fin structure holds the adsorbent granulate. In this work, two different sorbents are used: silica gel 123 with a radius of r_{SG} = 0.45 mm and zeolite 13X with r_{zeolite} = 0.7 mm. Due to the different density of the granulate, the adsorber heat exchanger can take 2.24 kg of silica gel and 1.83 kg of zeolite.

The heat exchanger of the evaporator is built from low finned copper tubes with an inner turbulence structure. The tubes are assembled horizontally in series. The low outer fins provide a thin water film by capillary action that leads to high heat transfer coefficients for evaporation (Xia et al. 2009). The resulting heat transfer coefficient is strongly dependent on the filling level and can be adjusted by altering the filling level of the evaporator (Lanzerath et al. 2014).

The condenser uses a simple spiral copper coil as heat exchanger that provides sufficient heat transfer area for the condensation process.

All components are heated and cooled with water circuits. For a specific operation condition, the evaporator and condenser are kept at constant temperatures whereas the adsorber is cycled between the adsorption and desorption temperature. The transferred heat flow is measured according to the following equation

$$\dot{Q} = \dot{V} \rho \, c \, (T_{\mathrm{in}} - T_{\mathrm{out}}) \tag{9}$$

where $\dot{V}$ is the volume flow of the water circuits and T_{in} and T_{out} are the temperatures at the inlet and outlet of the heat exchangers. Furthermore, the pressure inside each vacuum vessel is logged during operation.

Integrating the heat flow over cycle time t_{cycle} yields the heat Q transferred in the components during one cycle. These amounts of heat are used to calculate the coefficient of performance (*COP*) and the volumetric cooling power (*VCP*) of the adsorption chiller:

$$COP = \frac{Q_{\mathrm{evap}}}{Q_{\mathrm{des}}}, \tag{10}$$

$$VCP = \frac{Q_{\mathrm{evap}}}{t_{\mathrm{cycle}}\, V}\ . \tag{11}$$

Q_{evap} is the heat of evaporation whereas Q_{des} consists of the heat required to heat up the adsorber and the heat needed for the desorption process. V denotes the total volume of the heat exchangers of evaporator, condenser and adsorber including the sorption material.

Measurement uncertainties result mainly from the uncertainty of the volume flow and temperature sensors (cf. Table 1). Error propagation for all derived values is calculated according to (JCGM 2008) and the uncertainties for *COP* and *VCP* are typically below 10%.

Model calibration

The model is calibrated for two different setups of the adsorption chiller to test the model flexibility and robustness. Thereby, not only different operation conditions are tested but also sorbent variations and heat exchanger modifications. For this purpose, the setup is modified with respect to the adsorbent material and the heat exchanger coefficient of the evaporator. The heat exchanger of the adsorber is the same for both setups, only the sorbent is exchanged. The first setup is run with 2.24 kg silica gel 123 and the second with 1.83 kg zeolite 13X. Besides the difference in mass, the equilibrium data, the effective heat transfer coefficient $(\alpha A)_{\mathrm{A}}$ and the diffusion coefficient D of both materials are strongly altered. The model is therefore adjusted by replacing the Dubinin function of the adsorbent and by re-calibrating the transport coefficients of the sorbent. Additionally, the filling level of the evaporator for the zeolite setup is changed resulting in an altered heat transfer coefficient $(\alpha A)_{\mathrm{E}}$ of the evaporation process that requires a new calibration of the evaporator.

Measurements for calibration were conducted at an evaporation temperature of 10°C and an adsorption and condensation temperature of 35°C. To realize similar loading differences for both adsorbent materials, the desorption temperatures were set to 90°C for silica gel and 140°C for zeolite. Volume flows in the water circuits and switching times of the valves are the same in both setups with a total cycle time of t_{cycle} = 1860 s.

The actual calibration is conducted by running the simulation with measured inlet temperatures T_{in} and volume flows $\dot{V}$ of all three water circuits as model inputs. The parameters f_{E}, f_{C}, $(\alpha A)_{\mathrm{E}}$, $(\alpha A)_{\mathrm{C}}$ can be

calibrated independently to avoid unphysical coupling between the models due to a simultaneous fitting. Thereby, the modular modeling approach is strengthened. Only the final calibration of the transport coefficients ($(\alpha A)_\mathrm{A}$, D) in the adsorber is conducted simultaneously to account for the coupled heat and mass transfer within the sorbent.

The parameters are calibrated by minimizing the root mean square deviation (*RMSD)* between the measured and simulated heat flow of all components i:

$$RMSD_\mathrm{i} = \sqrt{\frac{1}{t_\mathrm{cycle}} \int \left(\dot{Q}_\mathrm{meas,i} - \dot{Q}_\mathrm{sim,i}\right)^2 \mathrm{d}t} \ . \tag{12}$$

Since the heat flows of the components can differ by more than one order of magnitude, the *RMSD* is weighted with the average absolute heat flow over a complete cycle yielding the coefficient of variation for each heat flow of component i:

$$CV_\mathrm{i} = \frac{RMSD_\mathrm{i}}{Q_\mathrm{i,meas}/t_\mathrm{cycle}} . \tag{13}$$

The final objective function for determining the calibration parameters is the average CV of the evaporator, condenser and adsorber:

$$CV = \frac{1}{3} \sum CV_\mathrm{i} \, . \tag{14}$$

The obtained calibration parameters can be found in Table 2. The friction factors f_E and f_C and the heat transfer coefficient $(\alpha A)_\mathrm{C}$ of the condenser are equal for both setups as the valves and the condenser are identical. The change of the filling level in the evaporator, in contrast, leads to an increase of the heat transfer coefficient $(\alpha A)_\mathrm{E}$ from 176 W/K to 384 W/K for the zeolite setup. Furthermore, the adsorber transport coefficients are different: the exchange of the sorbent causes a difference of factor 2 in the heat transfer coefficient $(\alpha A)_\mathrm{A}$ regardless of the fact that the heat exchanger itself remains the same. The diffusion coefficients differ significantly, too. For silica gel, the coefficient is the same for adsorption and desorption phase whereas for zeolite it is one order of magnitude higher for the desorption phase. The temperature dependence of diffusion is often expressed by the Arrhenius equation, but simulation with constant diffusion coefficients during the adsorption/desorption phases showed better results. It should be mentioned that the sorbent transport coefficients $(\alpha A)_\mathrm{A}$ and D are strongly interdependent and a high heat transfer coefficient can compensate a low diffusion coefficient and vice versa (see Figure 3). Therefore, the confidence level of

the sorbent transport coefficients is quite low. Despite this fact, the achieved model accuracy is impressive. For the silica gel setup, an average CV_{SG} as low as 13.3 % is reached and the average $CV_{zeolite}$ of 21.7 % for the zeolite setup is also very low (Table 2).

To get an impression of the simulation accuracy, Figure 4 shows the measured and simulated heat flow of the evaporator for both setups. In case of the silica gel setup, the simulated heat flow of the evaporator almost perfectly fits the measured values. The differences between simulation and measurement are within the noise of the measurement signal. This accuracy corresponds to a $CV_{E,SG}$ of 9.1%. The coefficient of variation for the zeolite setup is twice as high (19.6 %) but the simulation still matches the measurement data to a large extent. Differences between measurement and simulation are only distinguishable at the peak but the process dynamics are captured well. Thus, the dynamics of an adsorption chiller can be described accurately by state of the art models with little geometry information by sound calibration of only few parameters with regard to the *RMSD*.

Model validation

The calibrated model is validated by predicting the system behavior in both setups at various operating conditions. It is important to note that the prediction performance is investigated without any further re-calibration of model parameters. The operation conditions of the adsorption chiller are altered in terms of cycle time and temperature levels:

- short cycle time: 900 s for the silica setup, 1200 s for the zeolite setup
- long cycle time: 3600 s
- low evaporation temperature: 5°C
- high evaporation temperature: 20°C
- low desorption temperature: 70°C for the silica setup, 120°C for the zeolite setup
- high desorption temperature: 110°C for the silica setup, 160°C for the zeolite setup
- low adsorption temperature: 25°C

The minimum cycle time of the zeolite setup is extended to 1200 s to allow for the larger temperature change of the zeolite adsorber. Desorption temperatures for both setups also differ to account for the different

sorbent materials. For all investigated operation conditions, the accuracy of simulation is expressed in terms of the average coefficient of variation *CV* (Table 3).

The *CV* values of the silica gel setup range between 12.6 % and 27.4 % (calibration: 13.3 %), for the zeolite setup between 22.6 % and 39.7 % (calibration: 21.7 %). As expected, the *CV* values of the calibration cycles are among the lowest *CV* within their setup, however, the short silica gel cycle exhibits the lowest *CV* value of all. To some extent, this is a numerical effect, since the short cycle time with higher average heat flows may promote low *CV* (cf. equation (13)). Correspondingly, long cycles favor high *CV* values. On average, the *CV* values for the zeolite setup are 1.5 times higher than for the silica gel setup. This might be due to higher temperature jumps in the adsorber and due to temperature dependencies of the transport coefficients that are not accounted for. The maximum *CV* values for both setups are about twice the calibration *CV* values but still provide good agreement between measurement and simulation which is evident in the performance prediction of the coefficient of performance *COP* and the volumetric cooling power *VCP*.

The prediction capabilities for *COP* and *VCP* are shown in Figure 5. All but one predicted *COP* values of the silica gel setup lie within the standard measurement deviation. The average deviation between measurement and simulation is as low as 7.2 % which emphasizes the remarkable prediction capability. In case of the zeolite setup, the deviation has an average of 18.7 % and exceeds the measurement uncertainty in many cases. Thus, the predicted *COP* values are systematically too high. Reason for the systematic deviation might be heat losses that are neglected but more relevant at the higher desorption temperatures of the zeolite setup.

The model's prediction capability of the *VCP* is excellent for all investigated operation conditions and both setups. Only few predicted values lie outside the standard deviation of the measurements in spite of strongly varying *VCP* values. The average deviation between measurement and simulation is 4.3 % and the maximum 12 % for all cases of both setups. This underlines the high accuracy of the model for a wide range of operation conditions and different system setups which is also reflected in low *CV* values.

Compared to previous work, the presented model reaches high prediction accuracy within a wide range of operation conditions and moreover, also for different system setups. Wang and Chua (2007a, 2007b), for example, encounter deviations up to 50 % between measurement and simulation of cooling power. Chen et al. (2010), in contrast, report good agreement between measured and simulated values with deviations for

COP and cooling power below 7 %. However, Chen et al. only slightly vary the evaporation temperature between 10°C and 20°C.

Optimization

Models with reliable performance prediction allow tailored development and improvement of adsorption chillers. For instance, the influence of optimized heat exchanges can be quantified to assess the advantages and potential development costs. Furthermore, with high precision models, optimal switching times for valves can be identified, which is particularly important for effective heat recovery processes (Gräber et al. 2011). Additionally, reliable full dynamic models allow to study the influence of sorbent properties. This renders the possibility to define tailored sorbent properties for different scenarios and predict realistic performance figures. Until now, studies on sorbent properties were limited to static approaches (Follin et al. 1996) (Teng et al. 1997) (Schmidt et al. 2003) (Lanzerath et al. 2011) that can only give rough estimations for idealized scenarios.

In this work, we show how the validated model can be used to improve the average cooling power of an adsorption chiller setup by optimizing process and design parameters. The considered process parameter is the cycle time which strongly influences the average cooling power. The design parameters we optimize are the sizes of adsorber, evaporator and condenser for a fixed total volume. All other parameters (e.g. the temperature levels) are kept constant for the optimization.

Procedure

The design parameters are optimized by a brute force approach: the size of the three heat exchangers (adsorber, evaporator and condenser) is varied by a parameter sweep. This guarantees finding the optimum configuration and allows detailed discussion of the results. For each configuration of the parameter sweep, the optimal cycle time is evaluated using an optimization method proposed by Gräber (2013).

The sizing of the three heat exchangers has only two independent variables due to the constant total volume:

$$V = V_{\mathrm{A}} + V_{\mathrm{E}} + V_{\mathrm{C}} = const. \tag{15}$$

The two remaining parameters are varied subject to the following conditions:

$$0 < V_{\mathrm{A}} < V\,, \tag{16}$$

$$0 < V_{\mathrm{E}} < V - V_{\mathrm{A}}\,. \tag{17}$$

The variation of the heat exchanger volume is implemented by varying the length of the heat exchangers in the model. As the outer radii of the heat exchangers is set by the geometry (cf. Figure 2) this is equal to varying the volume. By changing the volume, the overall thermal conductance of the heat exchanger is also altered and almost proportional to the volume. There are only slight deviations due to the temperature dependency of the convective heat transfer inside the tubes.

For each configuration, the cycle time is optimized regarding the *VCP*. This is important for a valid comparison of the different configurations since the cooling power is strongly dependent on the cycle time. Long cycles promote the *COP* whereas short cycles promote the *VCP* (San and Tsai 2014). However, the *VCP* has a distinct maximum. For steady state operating conditions, Gräber (2013) found that the optimal length of the adsorption phase regarding the *VCP* is reached when the average cooling power exceeds the current cooling power:

$$\frac{1}{t_{\mathrm{ads}}}\int_0^{t_{\mathrm{ads}}} \dot{Q}_{\mathrm{E}}\,\mathrm{d}t > \dot{Q}_{\mathrm{E}}\,. \tag{18}$$

To ensure a symmetric operation characteristic, the length of desorption phase equals the length of adsorption phase. Additionally, switching of the vacuum valves in the isosteric heating and cooling phase is pressure controlled and thus no optimization parameter.

The optimization of the adsorption chiller design and the cycle time is conducted for both setups (silica gel and zeolite) at calibration conditions: evaporation at 10°C, adsorption and condensation at 35°C and desorption at 90°C (silica gel) and 140°C (zeolite), respectively. To assure equal conditions for the simulation of each configuration, we apply ideal and constant process conditions (i.e. inlet temperatures and volume flows) in the model by connecting the heat exchangers to ideal heat sources/sinks.

Results

Before optimizing the system design, the cycle time for the original experimental setup (V_{A} = 86 %, V_{E} = 9 % and V_{C} = 5 %) is optimized using equation (18) leading to optimal cycle times of 393 s for the silica gel

and 312 s for the zeolite setup. This is a reduction by approximately a factor of 4 compared to the initial cycle time of 1860 s. By this measure, the *VCP* is enhanced from 29 to 42 kW/m³ for silica gel and from 38 to 80 kW/m³ for zeolite. However, the higher *VCP* is achieved at cost of a significantly reduced *COP* compared to the longer cycles. For the silica gel setup the *COP* drops from 0.36 to 0.16, and for the zeolite setup from 0.26 to 0.13.

Figure 6 shows the results of the adsorption chiller design optimization by plotting iso-*VCP* curves. The three axes show the volume fraction of the adsorber, evaporator and condenser. The best design point is marked by an "x", the original setup by an "o". The bottom area in the graphs contains configurations with small evaporators. Operation with too small evaporators leads to freezing of the water and results in a sharp drop of the *VCP*. A similar behavior can be observed for configurations with small condensers (right region of the graphs). At some threshold, the condenser becomes too small to achieve full condensation resulting in a sharp decrease of the *VCP*. For configurations with small adsorbers (left side of the graphs) the cooling power decreases smoothly.

For zeolite 13X, the original design is very close to the VCP optimum. The optimum case employs a slightly larger evaporator (10 % volume fraction instead of 9 %) at expense of the adsorber. Accordingly, the *VCP* and the *COP* for the optimal design differ only marginally from the existing design. As the best design point lies in the lower right corner of the graph, this design is vulnerable to freezing: small changes in operating conditions (lower evaporation temperature or higher desorption temperature) may lead to malfunction of the adsorption chiller. Thus, an alternative sizing of the components may be chosen for more reliable operation of the chiller.

For the silica gel case, the optimal design leads to a *VCP* of 46 kW/m³ (+10 %). This design consists of a smaller adsorber with a volume fraction of 78 % and an increased evaporator with 19 % volume fraction. The condenser takes only 3 % of the total volume. This shift compared to the zeolite case can be explained by the lower evaporator heat transfer coefficients and the higher adsorber heat transfer coefficient of the silica gel setup (cf. Table 2). Since the adsorption potential of silica gel is lower, freezing in the evaporator is less probable.

Both optimizations show that the cycle time is a crucial process parameter concerning the *VCP* and must be considered while optimizing the system design. Furthermore, in a good design, the adsorber takes the

largest volume fraction with approximately 80 %. This result is mainly caused by the volume of the adsorption material and the relatively low heat transfer coefficient resulting in a large adsorber heat exchanger. The highest impact to increase the *VCP* of an adsorption chiller is therefore the adsorber heat exchanger design. By using high performance evaporators as in the zeolite setup, the volume share of the evaporator can be further reduced significantly to promote larger adsorbers and better usage of the available volume.

The presented optimization framework allows well-balanced design of adsorption heat pumps that can be very useful in designing future heat pumps, especially when considering coated adsorbers with high heat transfer coefficients that will shift the optimum design point to higher volume fractions of evaporator and condenser.

Conclusions

In this work, a dynamic state of the art model of an adsorption chiller is presented. The model was experimentally calibrated for two different adsorption chiller setups and extensively validated at various process conditions. The model incorporates only little geometry information and calibration parameters. The parameters are calibrated with respect to the root mean square deviation (*RMSD)* of the heat flows in all units. By this sound calibration not only qualitative but also excellent quantitative agreement for coefficient of performance (*COP*) and the volumetric cooling power (*VCP*) is achieved for all cases. More importantly, dynamic variables such as component temperatures and heat flows are very well predicted and the model accuracy is mathematically quantified. Thereby, the developed dynamic model is valid for a broad range of operating conditions and even for different adsorbent materials. This robustness allows a reliable component-wise optimization of adsorption chillers that is demonstrated by optimizing the sizing of the heat exchangers and the cycle time. It is shown that the cycle time influences the volumetric cooling power (*VCP*) significantly and that the adsorber is the most important component with a volume fraction of more than 80 %. By optimizing cycle time and sizing of the silica gel setup, the *VCP* is improved by 58 % to 46 kW/m³. Thereby, the modular experimental and simulation framework enables the systematic development of future adsorption systems.

Nomenclature

A	area (m^2)
α	heat transfer coefficient ($W\ m^{-2}\ K^{-1}$)
c	specific heat capacity ($J\ kg^{-1}K^{-1}$)
COP	coefficient of performance (-)
CV	coefficient of variation (-)
D	diffusion coefficient ($m^2\ s^{-1}$)
f	friction factor (m^{-1})
h	specific enthalpy ($J\ kg^{-1}$)
$\dot{H}$	enthalpy flow (W)
m	mass (kg)
$\dot{m}$	mass flow ($kg\ s^{-1}$)
μ	dynamic viscosity (Pa s)
p	pressure (Pa)
Q	heat (J)
$\dot{Q}$	heat flow (W)
r	radius (m)
ρ	density ($kg\ m^{-3}$)
$RMSD$	root mean square deviation (W)
t	time (s)
T	temperature (°C)
ΔT	temperature difference (K)
U	internal energy (J)
u	specific internal energy ($J\ kg^{-1}$)
v	velocity ($m\ s^{-1}$)
V	volume (m^3)
VCP	volumetric cooling power ($kW\ m^{-3}$)

x	loading (-)

Subscripts

A	adsorber
ad	adsorbed
ads	adsorption (phase)
C	condenser
des	desorption (phase)
E	evaporator
evap	evaporation
eq	equilibrium
i	place holder for A, C or E
in	inlet
l	liquid
meas	measured
out	outlet
SG	silica gel
sim	simulated
sor	sorbent
v	vapor

References

Bau, U., Lanzerath, F., Gräber, M., Graf, S., Schreiber, H., Thielen, N. and Bardow, A. 2014. Adsorption library modeling adsorption based chillers, heat pumps, thermal storages and desiccant units. *Proceedings of the International Modelica Conference*.

Chen, C.J., Wang, R.Z., Xia, Z.Z. and Kiplagat, J. K. 2010. Study on a silica gel-water adsorption chiller integrated with a closed wet cooling tower. *International Journal of Thermal Sciences*, 49(3):611-620.

Douss, N., Meunier, F.E. and Sun, L.-M. 1988. Predictive model and experimental results for a two-adsorber solid adsorption heat pump. *Industrial & Engineering Chemistry Research*, 27(2):310-316.

Dubinin, M.M. 1967. Adsorption in micropores. *Journal of Colloid and Interface Science*, 23(4):487-499.

Farid, S., Billah, M., Khan, M., Rahman, M. and Sharif, U.M. 2011. A numerical analysis of cooling water temperature of two-stage adsorption chiller along with different mass ratios. *International Communications in Heat and Mass Transfer*, 38(8):1086-1092.

Follin, S., Goetz, V. and Guillot, A. 1996. Influence of microporous characteristics of activated carbons on the performance of an adsorption cycle for refrigeration. *Industrial & Engineering Chemistry Research*, 35(8):2632-2639.

Fritzson, P. 2004. Principles of Object-Oriented Modeling and Simulation with Modelica 2.1. *John Wiley & Sons*.

Glueckauf, E. 1955. Theory of Chromatography. 10. Formulae for Diffusion into Spheres and their Application to Chromatography. *Transactions of the Faraday Society*, 51(11):1540-1551.

Gräber, M. 2013. Energieoptimale Regelung von Kälteprozessen. Ph.D. dissertation, TU Braunschweig

Gräber, M., Kirches, C., Bock, H.G., Schlöder, J.P., Tegethoff, W. and Köhler, J. 2011. Determining the optimum cyclic operation of adsorption chillers by a direct method for periodic optimal control. *International Journal of Refrigeration*, 34(4):902-913.

Gräber, M., Kosowski, K., Richter, C. and Tegethoff, W. 2010. Modelling of heat pumps with an object-oriented model library for thermodynamic systems. *Mathematical and Computer Modelling of Dynamical Systems*, 16(3):195-209.

JCGM. 2008. Evaluation of measurement data — Guide to the expression of uncertainty in measurement.

Khan, M., Alam, K., Saha, B.B., Hamamoto, Y., Akisawa, A. and Kashiwagi, T. 2006. Parametric study of a two-stage adsorption chiller using re-heat - The effect of overall thermal conductance and adsorbent mass on system performance. *International Journal of Thermal Sciences*, 45(5):511-519.

Khan, M., Alam, K., Saha, B., Akisawa, A. and Kashiwagi, T. 2007. Study on a re-heat two-stage adsorption chiller - The influence of thermal capacitance ratio, overall thermal conductance ratio and adsorbent mass on system performance. *Applied Thermal Engineering*, 27(10):1677-1685.

Lanzerath, F., Erdogan, M., Steinhilber, M. and Bardow, A. 2014. Combination of finned tubes and thermal coating for high performance water evaporation in adsorption heat pumps. *Proceedings of the International Sorption Heat Pump Conference*.

Lanzerath, F., Klitzing, B. and Bardow, A. 2011. Towards Tailored Materials for Adsorption Heat Pump Application, *Proceedings of the International Sorption Heat Pump Conference*.

Miyazaki, T., Akisawa, A. and Saha, B.B. 2010. The performance analysis of a novel dual evaporator type three-bed adsorption chiller. *International Journal of Refrigeration*, 33(2):276-285.

Saha, B.B., Boelman, E.C. and Kashiwagi, T. 1995. Computational analysis of an advanced adsorption-refrigeration cycle. *Energy*, 20(10):983-994.

Saha, B., El-Sharkawy, I., Koyama, S., Lee, J. and Kuwahara, K. 2006. Waste heat driven multi-bed adsorption chiller: Heat exchangers overall thermal conductance on chiller performance. *Heat Transfer Engineering*, 27(5):80-87.

San, J.-Y. and Tsai, F.-K. 2014. Testing of a lab-scale four-bed adsorption heat pump. *Applied Thermal Engineering*, 70(1):274-281

Santori, G., Sapienza, A. and Freni, A. 2012. A dynamic multi-level model for adsorptive solar cooling. *Renewable Energy*, 43(0):301-312.

Schawe, D. 2001. Theoretical and Experimental Investigations of an Adsorption Heat Pump with Heat Transfer between two Adsorbers. Ph.D. dissertation, Universität Stuttgart.

Schicktanz, M. and Nunez, T. 2009. Modelling of an adsorption chiller for dynamic system simulation. *International Journal of Refrigeration*, 32(4):588-595.

Schmidt, E.F. 1967. Wärmeübergang und Druckverlust in Rohrschlangen. *Chemie Ingenieur Technik*, 39(13):781-789.

Schmidt, F.P., Luther, J. and Glandt, E. D. 2003. Influence of Adsorbent Characteristics on the Performance of an Adsorption Heat Storage Cycle. *Industrial & Engineering Chemistry Research*, 42(20):4910-4918.

Teng, Y., Wang, R.Z. and Wu, J.Y. 1997. Study of the fundamentals of adsorption systems. *Applied Thermal Engineering*, 17(4):327-338.

Thome, J.R. 2010. Engineering Data Book III, Wolverine Tube, Inc.

Tso, C., Chao, C.Y. and Fu, S. 2012. Performance analysis of a waste heat driven activated carbon based composite adsorbent – Water adsorption chiller using simulation model. *International Journal of Heat and Mass Transfer*, 55(25–26):7596-7610.

Verde, M., Cortés, L., Corberán, J., Sapienza, A., Vasta, S. and Restuccia, G. 2010. Modelling of an adsorption system driven by engine waste heat for truck cabin A/C. Performance estimation for a standard driving cycle. *Applied Thermal Engineering*, 30(13):1511-1522.

Wang, X. and Chua, H.T. 2007a. A comparative evaluation of two different heat-recovery schemes as applied to a two-bed adsorption chiller. *International Journal of Heat and Mass Transfer*, 50(3-4):433-443.

Wang, X. and Chua, H.T. 2007b. Two bed silica gel-water adsorption chillers: An effectual lumped parameter model. *International Journal of Refrigeration*, 30(8):1417-1426.

Xia, Z.Z., Yang, G.Z. and Wang, R.Z. (2009). Capillary-assisted flow and evaporation inside circumferential rectangular micro groove. *International Journal of Heat and Mass Transfer*, 52(3-4):952-961.

Zhang, G., Wang, D., Zhang, J., Han, Y. and Sun, W. 2011. Simulation of operating characteristics of the silica gel–water adsorption chiller powered by solar energy. *Solar Energy*, 85(7):1469-1478.

Tables

Table 1: Average measurement values and standard uncertainty of the volume flow and temperature sensors for the calibration cycle of the silica gel setup

	volume flow (l/min)			temperature difference (K)		
	evaporator	**condenser**	**adsorber**	**evaporator**	**condenser**	**adsorber**
average value	11.5	6.7	10.0	0.230	0.421	1.764
uncertainty	0.195	0.191	0.026	0.017	0.017	0.029

Table 2: Calibration parameters (cf. Figure 1) and model accuracy (eq. (14)) for the silica gel and zeolite setup

	calibration parameters							model accuracy			
setup	f_C	f_E	$(\alpha A)_C$	$(\alpha A)_E$	$(\alpha A)_A$	D_{ads}	D_{des}	CV_E	CV_C	CV_A	CV
	(m^{-1})	**(m^{-1})**	**(W/K)**	**(W/K)**	**(W/K)**	**(m^2/s)**	**(m^2/s)**	**(%)**	**(%)**	**(%)**	**(%)**
Silica gel	151e3	300e3	3174	176	331	1.8e-10	1.8e-10	9.1	16.8	14.0	13.3
zeolite				384	142	3.4e-10	2.8e-09	19.6	19.2	26.2	21.7

Table 3: Average coefficient of variation *CV* values (Eq. 14) for all investigated operation conditions in %

	calibra-tion	**short cycle**	**long cycle**	**low evap temp**	**high evap temp**	**low des temp**	**high des temp**	**low ads temp**
silica gel	13.3	12.6	22.1	16.6	22.2	27.4	21.6	17.5
zeolite	21.7	28.0	39.7	23.1	29.3	22.6	33.6	38.4

Figures

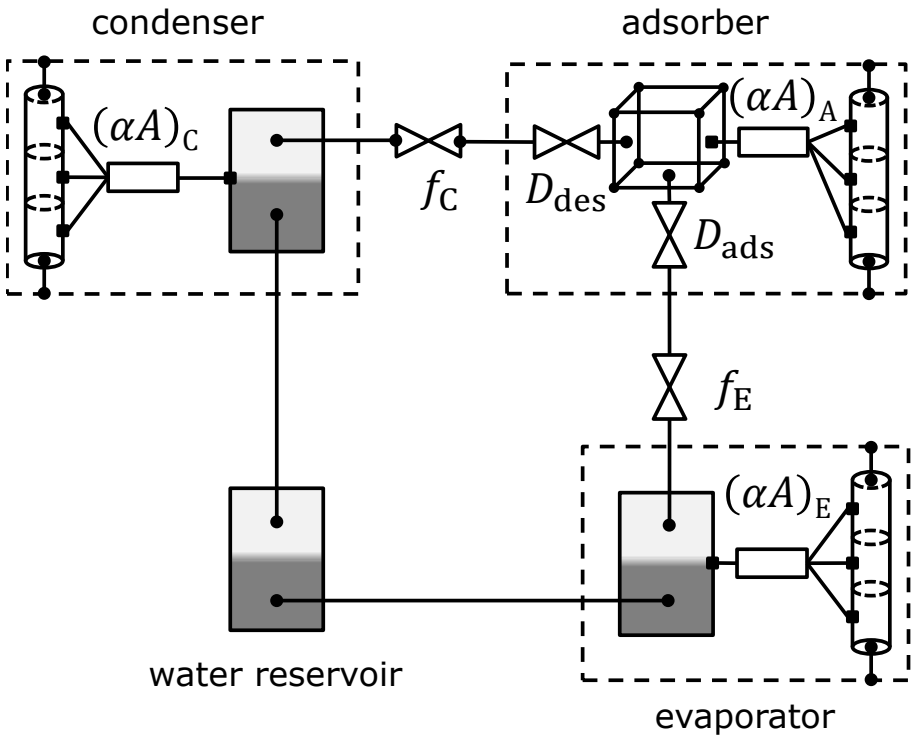

Figure 1: Model structure of the adsorption chiller with all fitting parameters

Figure 2: Heat exchangers of adsorber, evaporator and condenser (from left to right)

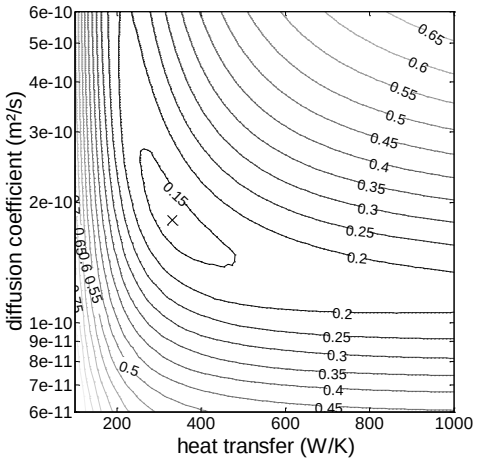

Figure 3: Contour plot of the average coefficient of variation *CV* (eq. (14)) as function of heat transfer coefficient $(\alpha A)_{\mathrm{A}}$ and diffusion coefficient D for the silica gel setup

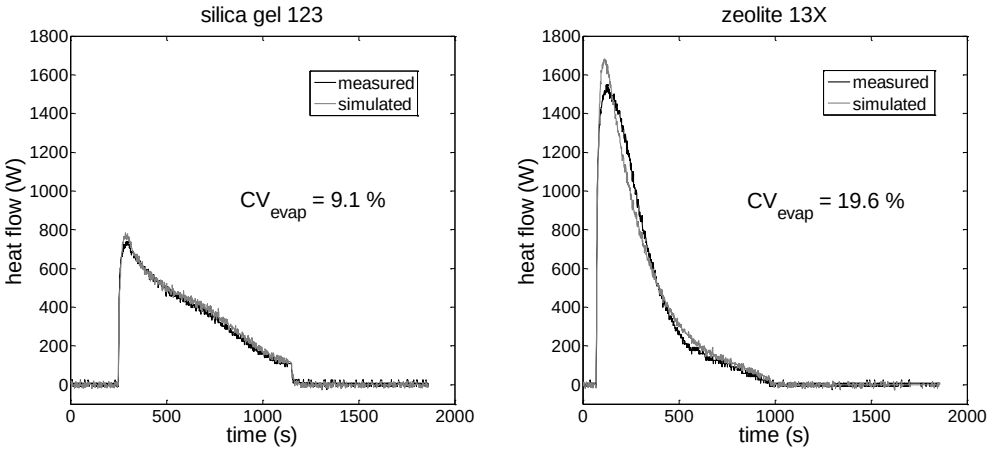

Figure 4: Measured and simulated heat flow of the evaporator for the calibrated cycles of the silica gel setup (left) and the zeolite 13X setup (right)

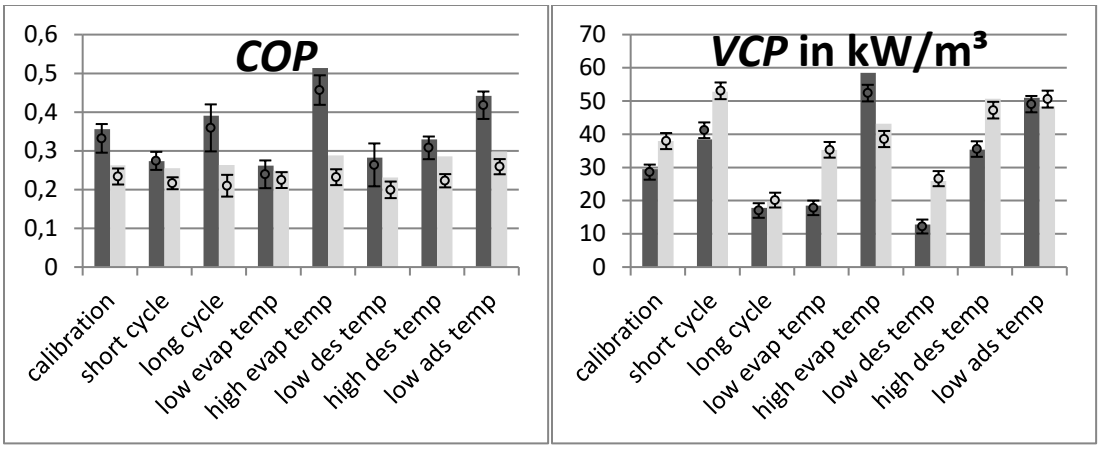

Figure 5: Prediction capability for coefficient of performance *COP* and volumetric cooling power *VCP* for silica gel 123 (dark) and zeolite (light). Simulation results (bars) are compared to measurement data (dots) with error bars indicating the uncertainty of measurement.

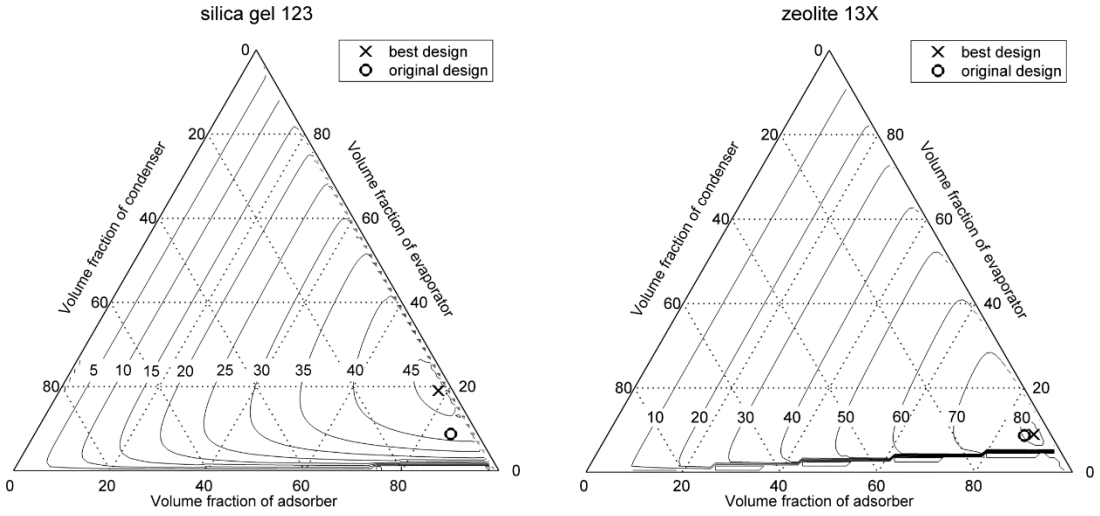

Figure 6: Contour plot of volumetric cooling power *VCP* for different adsorption chiller designs for silica gel 123 (left) and zeolite 13X (right) for optimized cycle times as a function of the volume fraction of adsorber, evaporator and condenser